

The heterogeneous substructure of casein micelles evidenced by SAXS and NMR in demineralized samples

Márcio H. Nogueira¹, Lucile Humblot¹, Raghvendra Pratap Singh¹, Emilie Dieude-Fauvel¹, Bertrand Doumert², Sarah Nasser³, Celine Lesur³, Romdhane Karoui⁴, Guillaume Delaplace¹, Paulo P. S. Peixoto¹

1 - Univ. Lille, CNRS, INRAE, Centrale Lille, UMR 8207 - UMET - Unité Matériaux et Transformations, équipe Processus aux Interfaces et Hygiène des Matériaux (PIHM), F-59000 Lille, France.

2 – Université de Lille, CNRS, INRA, Centrale Lille, ENSCL, Université d'Artois, FR 2638 - Institut Michel - Eugène Chevreul (IMEC), France

3 - Ingredia Dairy Experts, Arras, France

4 - Institut Charles Viollette (ICV), Université d'Artois, INRAE, ISA Lille, ULCO, Université de Lille, Lens, F-62300, France - ADRIANOR, Tilloy Les Mofflaines, F-62217, France

ABSTRACT

The casein micelle (CM) have been described as a protein assembly held together by interactions between phosphoryl groups from the protein moieties, and several internal calcium phosphate nanoclusters (CCPs). While the presence of protein inhomogeneities at the small scale, sequestering the CCPs, has been widely accepted, the presence of medium scale inhomogeneities, the so-called “Hard” regions, and its relationship with the CCPs, has been object of debate. In the present work, solid state NMR and SAXS data have been combined to study the correlation between the removal of CCPs and the structural modification of the micelle. A «native» sample and three different demineralized ones; 5% (DM-05), 10% (DM-10), and 25% (DM-25) of calcium in relation with the «native», have been analyzed. NMR data show that the reduction in the total amount of calcium and phosphorous ions (-5%, -10% and -25% respectively) in the samples is not always equivalent to the loss of CCPs as measured by the decrease of the amount of colloidal ³¹P (-15 and -17% and -25% respectively) in the samples. NMR data also indicate, that demineralization induces the total depletion of some CCP while leaving the remaining cluster in a rather «native» like structure. SAXS data show a good correlation between the amount of ³¹P loss measured by NMR and the decreases in intensity for the SAXS spectral features associated with the nanoclusters. Finally, SAXS data show the demineralization induces a decrease in the amount of the larger inhomogeneities in the micelle (the so called “Hard” regions). However, this decrease is not directly correlated to the decrease in the amount of CCPs (as measured by SAXS and NMR) indicating that these “Hard” regions may be, at least partially, maintained by a large protein-protein interaction network. The data and results are discussed and compared with different structural models of casein micelle.

Keywords: Casein micelle nanostructure, demineralization, calcium phosphate clusters, NMR.

1 INTRODUCTION

The casein proteins are primary constituent in cow's milk and represent ~80% of total protein content. These proteins are associated with colloidal calcium phosphate (CCP) into major molecular assembly present in the cow's milk and most of the dairy products called casein micelles (Walstra et al., 2006). The micellar casein presents excellent digestibility, higher amino acids supplement and especially leucine (Vickery & White, 1933). Because of its industrial and dietary importance, the characteristics and relation between its structure and the physico-chemical environment have been widely studied (Beliciu et al., 2012; Crowley et al., 2014; Dahbi et al. 2010; Silva et al. 2013).

The calcium phosphate nanoclusters play a pivotal role as a molecular glue in the casein's assembly into casein micelle (De Kruif & Holt, 2003). The casein micelles show high degree of dissociation upon loss of calcium phosphate and if the loss of calcium phosphate is >45%, it induces the formation of caseinate (Bouchoux et al., 2009; Ingham et al., 2016). While the partial loss (between 5%-45%) of CCP induces internal restructuring of CMs (Boiani et al., 2018; Broyard & Gaucheron, 2015; Kort et al., 2011; McCarthy et al., 2017; Ramchandran, Luo, & Vasiljevic, 2017) but no major changes have been observed in the micellar size (~5%) (Ingham et al., 2016).

Despite the studies done towards understanding the role of CCPs in details, the influence of CCPs in micellar caseins is still a matter of debate among scientific community. The recent studies by De Kruif et al. (2014) supports the so called "Nanocluster Model" of casein micelles (figure 1). In this model, as proposed by De Kruif et al. (2014), the CCPs are presented as central body covered by their protein counterparts (caseins) and many of such small assemblies are clustered together via the interaction of the free dangling tail part of the caseins to the neighboring assemblies (figure 1). The small-angle x-ray scattering (SAXS) and Neutron scattering (SANS) data support this "Nanocluster Model" of CMs assembly. Among other features, SANS data show that the composition of micelles is quite homogenous at the medium size scale (>10nm) but inhomogeneities are observed near the small size scale of ~4nm.

The work of Bouchoux et al. (2010) proposed a complexification of the model (we will call here the sponge-model) at the medium scale range. This work shows that the CMs are composed of several domains of ~20nm in size (called "Hard" regions) formed by protein assemblies to CCPs or free protein assemblies without CCPs and

water cavities of similar sizes. Their data show that, under osmotic stress, the casein micelles are compressed as a sponge, while some regions (attributed to the presence of large voids) collapse first leaving unchanged the so called “Hard” regions in the first degree of compression. The presence of these inhomogeneities contrasts to what have been stated by De Kruif, C. G. (2014); that the micelle is homogenous gel at the medium size scale. Such homogenous gels in the size scale of tens of nanometers, as presented by the “Nanocluster Model”, should display a continuous variation of the internal structure of the micelle as a function of the reduction of the micellar volume.

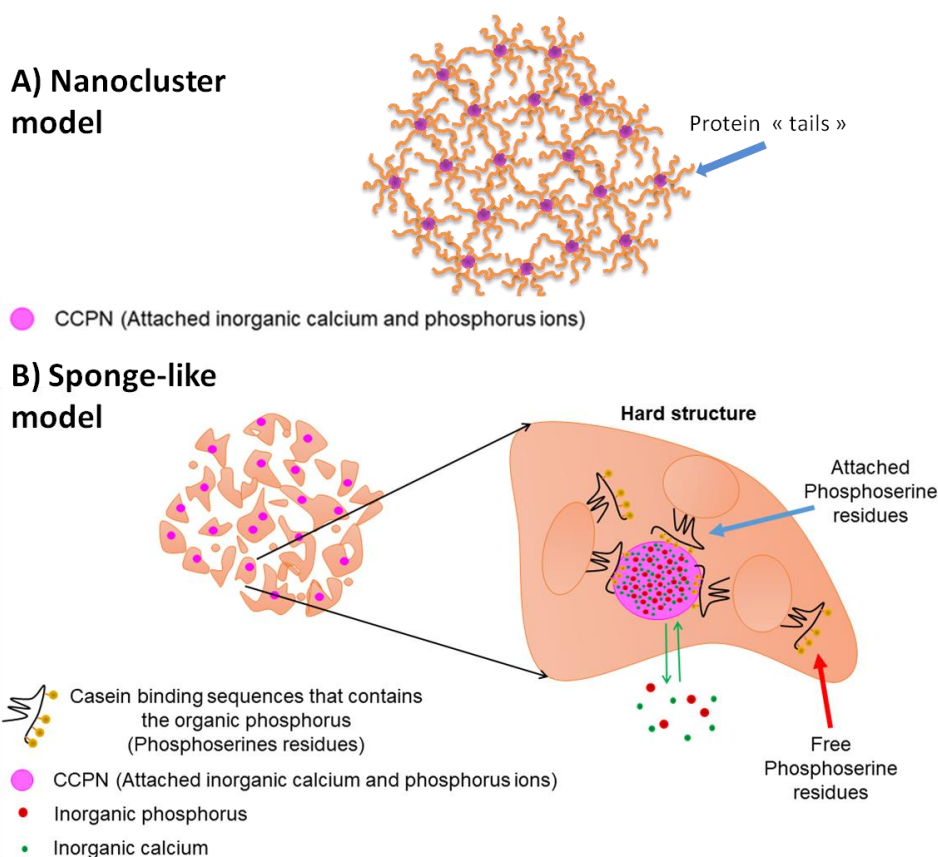


Figure 1 – (A) Schematic representation of the so-called nanocluster model as proposed by De Kruif, C. G. (2014): a casein micelle formed by small nanocluster units composed of a CCP and shell of proteins where the tails of these proteins interact with the neighbor nanoclusters. (B) Schematic representation of a CM as proposed by the “sponge-like model”. (Right) Zoom into a so-called “Hard” region representing casein micelles binding sequences (phosphoserine residues) interaction with calcium phosphate nanoclusters (CCP) through organic phosphorous from phosphoserine residues. Green arrows represent the equilibrium between calcium and phosphorous ions between the CCP (Colloidal phase) and the soluble phase. One can notice that all nanoclusters (CCP) are “enveloped” by proteins represented in brown (which constitutes the “hard” structures).

In the present work, the primary objective is to fill in the gaps between aforementioned models and data, also to better understand and provide new insights towards the role of CCPs in the casein micelle's structure and dynamics. To achieve the set goals, this study has associated SAXS data with ^{31}P solid state nuclear magnetic resonance (NMR) to understand and improve the knowledge regarding the specific impact of different degrees of demineralization on the local structure of clusters. Moreover, fluorescence spectroscopy has been used to better understand how hydrophobic interactions between proteins evolve with the different levels of demineralization.

2 MATERIALS AND METHODS

2.1.1 Samples identification

The casein-based powders studied in this work were manufactured and supplied by Ingredia S.A (Arras, France). The powders were produced at industrial pilot plant of Ingredia using traditional drying procedures (Pierre et al., 1992; Schuck et al., 1994).

The powders were mostly composed of casein proteins and over 82% (w/w) of protein content proof was reported by Ingredia, representing over 90% of the total nitrogen content from powders (see Table 1, SI). Four different compositions of powders at different degree of demineralization were used in the present study,

- 0% calcium-demineralized powder (from here on “«native»”) was used as control,
- 4.47% calcium-demineralized powder (DM-05),
- 9.16% calcium-demineralized powder (DM-10),
- 25.73% calcium-demineralized powder (DM-25),

The four powder formulations were identified as described previously as the closest to the real demineralization values (rounded off to the real demineralization value). It is also important to mention that the process used to generate and rehydrate all the powders, might have some impact on the structure of casein micelles (Nogueira

et al., 2020). For this reason, the «native» sample will always be displayed within quotation marks.

2.1.2 Demineralization and powder production

To produce such calcium-demineralized CM-rich powders, one starts from acidified skimmed milk at three different pHs (6.4, 6.2 and 5.9) using lactic acid. This process allows the excision of certain percentage of calcium from CMs, as described in literature (Broyard & Gaucheron, 2015).

The calcium-demineralized CMs-rich powders start from skimmed milk, which was acidified to three different pHs (6.4; 6.2; and, 5.9) by the addition of lactic acid. This process permits the excision of part of the calcium from the CMs, as described by the literature (Broyard & Gaucheron, 2015).

The present study follows the protocol applied by Silva et al., (2013), which reports a decrease of about 6%, 14% and 23% of the total calcium from CMs concentrates, which was acidified with hydrochloric acid and to three pH values of 6.4, 6.1 and 5.8. To ensure that the complete equilibrium is achieved, the acidified skimmed milk was left at 10°C for 10hours (maturation time).

The maturation time is followed by a protein concentration step, which consists of ultrafiltration process with a membrane cut-off of 10 kDa. The ultrafiltration process concentrates the milk proteins via the selective removal of water and soluble salts (Carvalho & Maubois, 2010). The protein concentrates are then submitted to membrane separation techniques, which follows two subsequent microfiltration. The first microfiltration was aimed at removing the bacterium and the membrane cut-off of 1.4µm was used, while the second microfiltration was performed with the 0.1µm pore size membrane to remove soluble constituents of the concentrates such as whey proteins, lactose and soluble minerals, which simultaneously concentrates the CMs at higher degree (Pierre et al., 1992).

2.1.3 Powder rehydration

The casein-rich powders were rehydrated with deionized water to 14.0 g (protein) x 100 g⁻¹ (water) submitted to stirring at 500 r.p.m at 50 °C/1 hour. Three drops of antifoam silicon solution were added to each powder dispersion at the

beginning of the rehydration to prevent the foam formation. The pH was adjusted to 7.0 with NaOH 1M. After pH adjustment, the samples were homogenized at 10000 r.p.m for 5 minutes using a rotor-stator homogenizer, Polytron PT 10-35a (Kinematica, France). Antimicrobial agent sodium azide was added to 0.3 g L^{-1} (Sigma Aldrich, France) to prevent microbiological growth.

2.1.4 Fluorescence measurements

To measure changes in the number of hydrophobic interaction in the CMs, the Fluorescence spectroscopy (using tryptophan as a probe) has been used. The Fluorescence analysis method used is the one used in our previous publication (Nogueira et al., 2020), using a Fluoromax-4 spectrofluorometer (Jobin Yvon, Horiba, NJ, USA). The angle of the excitation radiation set at 60° and temperature controlled by Haake A25 AC200 temperature controller set to 20° C (Thermo-Scientific, Courtaboeuf, France). The samples were poured into a 3 mL quartz cuvette and the emission spectra of tryptophan residues in a wavelength from 305 to 450 nm after excitation set at 290 nm were analyzed.

2.1.5 CMs structure organization observed by Small-angle X-ray scattering (SAXS)

In the present study, the SAXS method was applied to investigate the structure of the CMs at different levels. As described in the literature (Bouchoux et al. 2010) the SAXS spectra of the CMs is representative of three levels, which correspond to different structures from the micelle: i) the level 0, which is the micellar envelope ($\sim 100 \text{ nm}$ of diameter) corresponding to a Q range 0.0065 to 0.0010 nm^{-1} and, in the present concentration, to the inter-micellar distance; ii) the level 1, which corresponds to smaller structures ($\sim 20 \text{ nm}$ of diameter) described as “Hard-regions”, which are related to incompressible structures (Ingham et al., 2016), once submitted to osmotic pressure, within the micelle corresponding to a Q range of 0.042 to 0.006 nm^{-1} ; and iii) the level 2, which arises mainly from the structure of proteins associated to CCP (Ingham et al., 2016), assigned to an apparent “shoulder-region” at a Q range between 0.042 to 0.27 nm^{-1} . The quantification of the intensity of this last “shoulder” have been

measured by averaging the SAXS intensity between 0.07 and 0.15 nm⁻¹ (the center of the “shoulder”) for each sample. The values in relative percentage are given in table 1.

The SAXS measurements were conducted as described in (Nogueira et al., 2020). All SAXS acquisitions were performed at room temperature (~25 °C) at the French national synchrotron facility SOLEIL in Gif-sur-Yvette, France; on the SWING beamline operating at ~12 keV of photon energy. The SAXS intensities were recorded on a detector placed at ~0.5 m and 6.5 m from the sample. For each sample, data was recorded at short exposure time (typically ~0.2 s) to prevent any radiation damage.

2.1.6 Nuclear Magnetic Resonance (NMR) Spectroscopy quantification of attached phosphoserines and nanoclusters phosphorous

The four different phosphorus species present (Boiani et al., 2016), (Peixoto et al., 2017), (Boiani et al., 2018) (Gonzalez-Jordan et al., 2015) in the CMs rich powder formulations based on their localization and interactions with the micellar components were analyzed and characterized by NMR method. The phosphorus species are identified into four classes based on which CMs part they belong to. The first species is the “Organic” phosphorus of phosphoserine amino acids attached to CCP cluster; the second species is also an “Organic” phosphorus of identical origin but not interacting with CCP clusters (more dynamic because of free phosphoserine residues); “inorganic” soluble phase phosphorus is classified as third species and “inorganic” phosphorus forming or bound to the CCP cluster is the fourth distinct species present in the CMs. Noteworthy, here the appellation of “free” (organic and inorganic) phosphorous refers the phosphorous that are linked to only one or multiple calcium ions (but not to a cluster) as well for the phosphorous in its anionic form since both of these forms (linked to calcium ions or not) are indistinguishable in the NMR spectra, in the present conditions. Indeed, the binding of calcium ions to a single phosphate is always much faster than the NMR measurement resulting in a peak that represents the average signal between these two species (linked to calcium ions or not).

The NMR analysis was conducted as described by Nogueira et al., (2020) using a Bruker AVANCE I; 9.4T (1H: 400 MHz; ³¹P: 161.9 MHz) spectrometer, which was used to measure the ³¹P spectra, proton (¹H), cross-polarization (CP) and the t1 (direct correlation between ³¹P and ¹H).

More specifically, Bruker AVANCE I; 9.4T (^1H : 400 MHz; ^{31}P : 161.9 MHz) spectrometer was used to measure the ^{31}P spectra, proton (^1H), cross-polarization (CP) and the t1 (direct correlation between ^{31}P and ^1H). The 4 mm probe heads were set with samples and submitted to 700 Hz of Magic Angle Spinning (MAS) speed. Quantitative experiments at 25°C of ^{31}P were done with high power decoupling- recycle delay: 30s; 90° pulse; RF field (^{31}P): 65 kHz; ^1H decoupling (RF field: 60 kHz; SPINAL64); 1024 accumulations. The chemical shifts were given in parts per million (ppm) concerning the analysis of H_3PO_4 (85%) for ^{31}P NMR spectra at 0ppm.

In the quantitative spectra, the area of the different peaks in the spectrum corresponds to the relative abundance of each phosphorus species obtained from the ^{31}P -NMR analysis. The NMR spectra was simulated using the DMFIT software (Peixoto et al., 2017; Massiot et al., 2002) to access the area of each peak that corresponds to the different species of phosphorus present, that forms the ^{31}P -NMR spectra, in the CMs dispersions. The peak's decomposition is presented in the (Figure1, SI). As a control for the demineralized samples, the signal from «native» sample was used, where 100% of the signal was considered as representative signal for the attached phosphoserine and CCP.

The peaks decomposition is presented in figure 1 in supporting information. The signal from the «native» sample used as representative of the 100% of the signal for the attached phosphoserine and CCP and was used as a control for the demineralized samples. The fit is made following a standardized protocol already described (Peixoto et al., 2017) based in a first step of manual fit followed by an automatic adjustment made by DMFIT software.

Concomitantly, a NMR ^1H - ^{31}P cross-polarization experiment have been made to study the calcium/phosphorous concentration in the CCP by studying the NMR signal of the organic phosphorous from the phosphoserines residues, attached to the CCP. The principle is that, in our conditions organic phosphorous from the phosphoserines residues display a chemical shift anisotropy (CSA) shape is sensitive to strength of the hydrogen bond network as well as the ionic environment of the phosphorous (Gardiennet-Doucet, Assfeld, Henry, & Tekely, 2006). The ^1H - ^{31}P cross-polarization experiments strengthen specifically the signal of the chemical shift anisotropy (CSA) signal of the attached phosphoserines phosphorous (in contrast to the signal of inorganic phosphorous that does not display a methyl proton at its close

environment) (Peixoto et al., 2017) and, by doing so, allows a better access the CSA parameter of the organic phosphorous.

2.1.7 Statistical analysis

The data presented in this study were analyzed using an analysis of variance (ANOVA) followed by a Tukey test at $p < 0.05$; and a principal component analysis was performed for the data from the fluorescence spectroscopy.

3 RESULTS and DISCUSSION

3.1 Demineralization impacts on the internal organization of the CMs structure

3.1.1 The stability of hydrophobic interactions evaluated through fluorescence spectroscopy

In the present study, no significant difference of fluorescence intensity, or λ -max (the wavelength at which the tryptophan of the samples exhibit the maximum of its absorbance), has been observed between the «native» CMs and the three calcium-demineralized CMs samples (Figure 3, SI).

These results demonstrate that in comparison to the «native» samples, even the most demineralized samples (DM-25) do not display a significant change in the molecular environment of the tryptophan. This indicates that demineralization does not have any significant effect on the hydrophobic interactions between proteins, **at least in the present level of demineralization**. The CCPs are attached to the hydrophilic or charged structures of the CMs, which are primarily composed of phosphoserine residues including some glutamate residues (Walstra et al., 2006). In our understanding, the demineralization that induces depletion of CCPs from the CMs is responsible for the changes in the charge and hydrophilic interactions between the internal proteins that form the CMs. In Literature (Horne, 2017).

3.1.2 Organic and inorganic ^{31}P distribution and the environment by NMR

Since CCPs act as a cross-linking centers in casein micelles, the decrease in the amount of CCP is an essential factor governing the CMs structure (De Kruif & Holt, 2003). The Calcium and phosphorous ions within the CCPs are in equilibrium with the ions in the soluble phase, and this equilibrium depends on the chelating properties of the local structure of the micelle (Bijl et al., 2019).

The ^{31}P -NMR spectra corresponding to the organic phosphorus from the free phosphoserine residues and inorganic phosphorus present in the soluble phase (free inorganic phosphorous) can be seen in figure 2. As it can be clearly observed, that

more demineralized is the sample (DM-25), the greater is the amount of free phosphoserine residues.

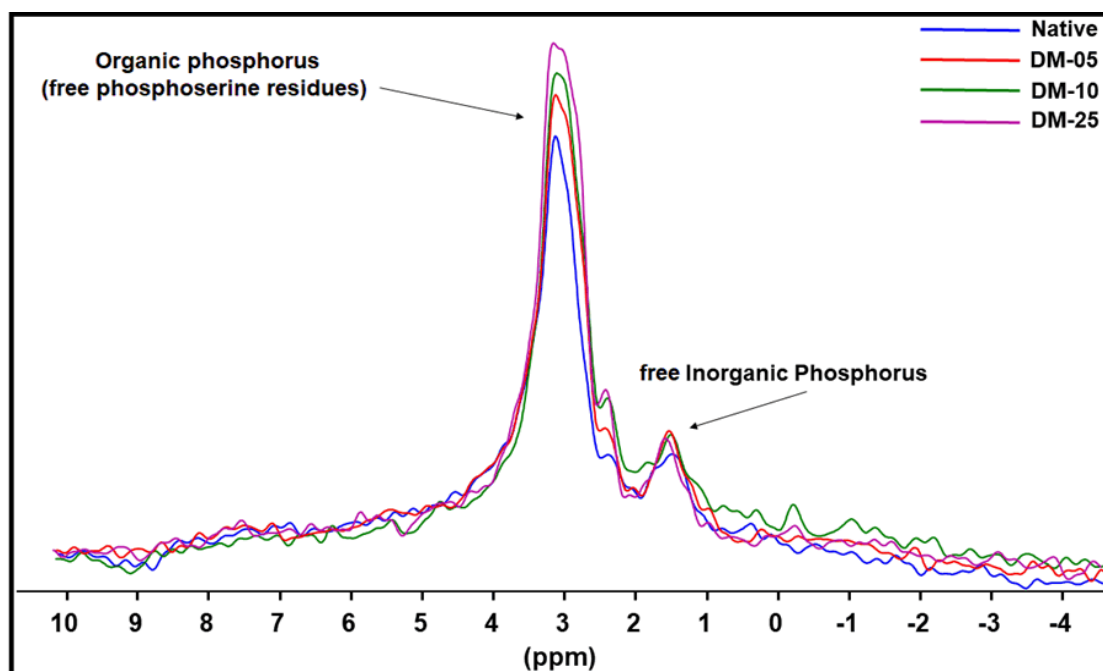


Figure 2 – Zoom in the region displaying the sharper peaks in the ^{31}P nuclear magnetic resonance (NMR) spectra from casein samples with different demineralization levels, being: («native») = »native« casein; (DM-05) = 4.47% demineralized casein; (DM-10) = 9.16% demineralized casein; (DM-25-25) = 25.73% demineralized casein.

Concomitantly to the increase in the number of free phosphoserine residues as observed represented in Figure 2, for the demineralized samples, a decrease in the number of attached phosphoserine residues (figure 3) and attached inorganic phosphorous is observed.

The decrease in the number of attached phosphoserines residues has been reported to be related to the loss of phosphoserine residues attached to the CCPs as a result of CM demineralization (Famelart et al., 2009). It is important to take into account that some amount of the measured free ^{31}P in all samples is likely to come from the κ -caseins' phosphorous which are not bound to CCP. In figure 3, it can be observed that the amount of inorganic attached phosphorus displays the same trends as the CCP.

Quantitatively, the results from ^{31}P -NMR (figure 3) reveals, that the decrease of attached phosphoserines and attached CCPs, as a function of demineralization display a nonlinear relation. As a function of the demineralization level, There is a more substantial loss of attached species (phosphoserine residues and CCP) for the less

demineralized samples than for the most demineralized sample. Indeed, the difference in the total calcium content between the «native» and the two less demineralized samples (DM-05 and DM-10) is only 5% and 10%, but this represents more than 15% and 17% of the loss in the attached inorganic phosphorus. In contrast, for the most demineralized sample (DM-25) the total loss in calcium content (-25%) is quite equivalent to the loss of attached inorganic phosphorus (CCP).

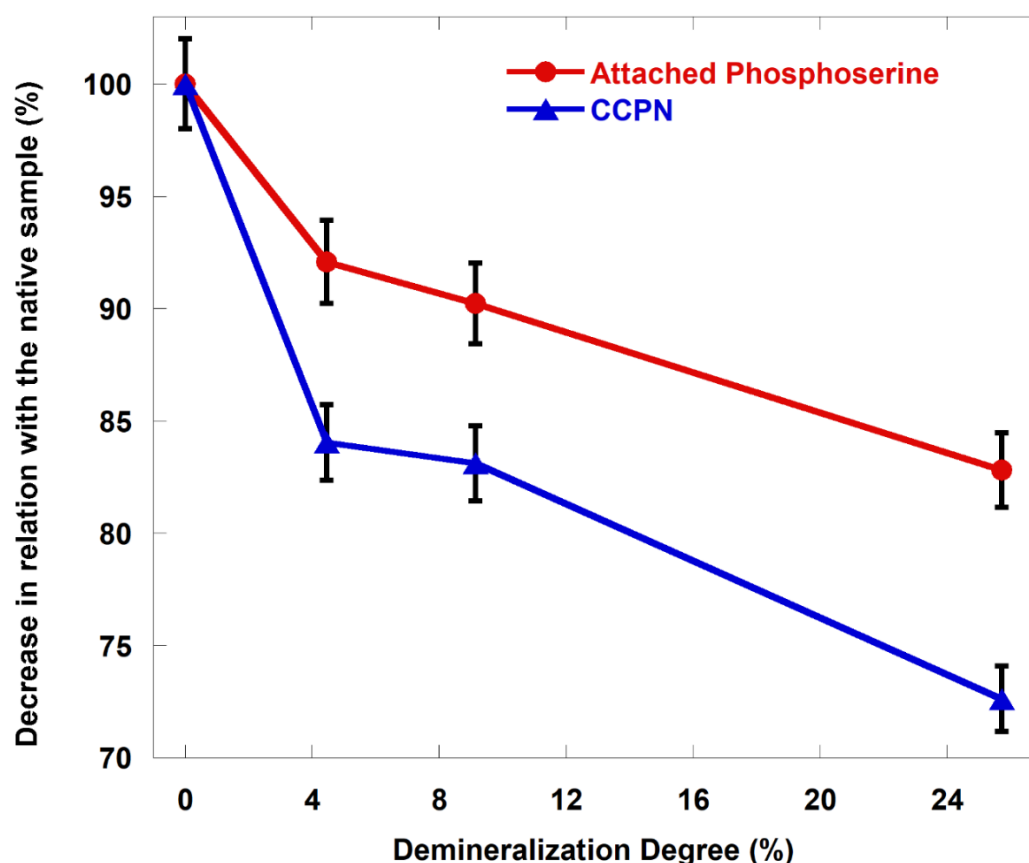


Figure 3 - Decrease in the number of attached phosphoserine (P-Ser) residues (●) and CCP (▲) as a function of the different demineralization degrees of casein dispersions. These results were obtained from the differences obtained from the fitting of the ^{31}P -NMR of a «native» casein micelle dispersion and three different degrees of demineralization (DM-05) 04.47% less calcium; (DM-10) 9.16% less calcium and (DM-25) 25.73% less calcium.

It is important to notice that in the first step (from DM-05 to DM-10) the loss of attached phosphoserines residues is less accentuated (about -7%) than the loss of CCP phosphorous (between -15-17%). In contrast, for the more demineralized samples the loss seems rather similar for both, phosphoserines and CCP phosphorous.

The present study is in accord with our previous work (Peixoto et al., 2017) and the signal of the attached phosphorus from the phosphoserine residues, displays a clear CSA (chemical shift anisotropy) shape (Figure 1, SI). As explained in the experimental section, the shape of the CSA is sensitive to strength of the hydrogen bond network around the phosphoryl oxygens as well as the close ionic environment (Gardiennet-Doucet et al., 2006). This makes the CSA signal highly informative about the proximity of cations as calcium around the phosphorous from the phosphoserines. The data presented in supporting information shows that demineralization induces only small changes in the CSA signal shape of attached phosphoserines suggesting that, even in strongly demineralized samples, most of the remaining CCP cluster keeps a near-«native» composition in terms of Ca/P ratio.

Since this last result indicates that, even in the most calcium-demineralized sample (DM-25), the Ca/P ratio in the CCP remains close to the «native» sample, the observed loss of inorganic phosphorus is likely to correspond to equal loss of calcium from the clusters. Thus, such result indicates that demineralization does not strongly affect the properties of the remaining clusters in the demineralized samples in terms of size and composition. Indeed, smaller clusters after the loss of about 25% of inorganic and organic phosphorous as displayed by our data should display a higher surface tension, which might impact the hydrogen bond network around the CCP. Instead, the data indicate that the remaining clusters in demineralized samples display a quite «native»-like order and composition. It is possible that a loss of only 15% of calcium phosphate ions in the clusters would not induce a detectable change in the H-hydrogen network around the surface of the cluster. However, it is unlikely that a loss superior to 25% of the ions would induce any detectable change in CSA, considering if this loss is homogenous for all clusters. Thus, the scenario more compatible with our data is that demineralization has induced a complete depletion of some clusters at least in the case of the most demineralized sample.

3.1.3 Internal structures reorganization evaluated through SAXS:

In this section, SAXS data analysis has been used to study the impact of demineralization over the cluster size, as well as over CM structures (~5 to 50 nm). Each “shoulder” of the SAXS profile (figure 4) can be assigned to a characteristic structure of the micelle (see details in the experimental section).

As it concerns level 2 proteins associated with the “sequestered” CCP (P-CCP), one can notice that demineralization induces some decrease in intensity of the corresponding “shoulder” (figure 4a corresponding to level two), but there is no detectable shift. This same feature have been observed in previous works in presence of calcium chelator agents or in lowering of pH (Ingham et al., 2016). Such feature is interpreted as a loss of local inomogenous protein structure around the cluster.

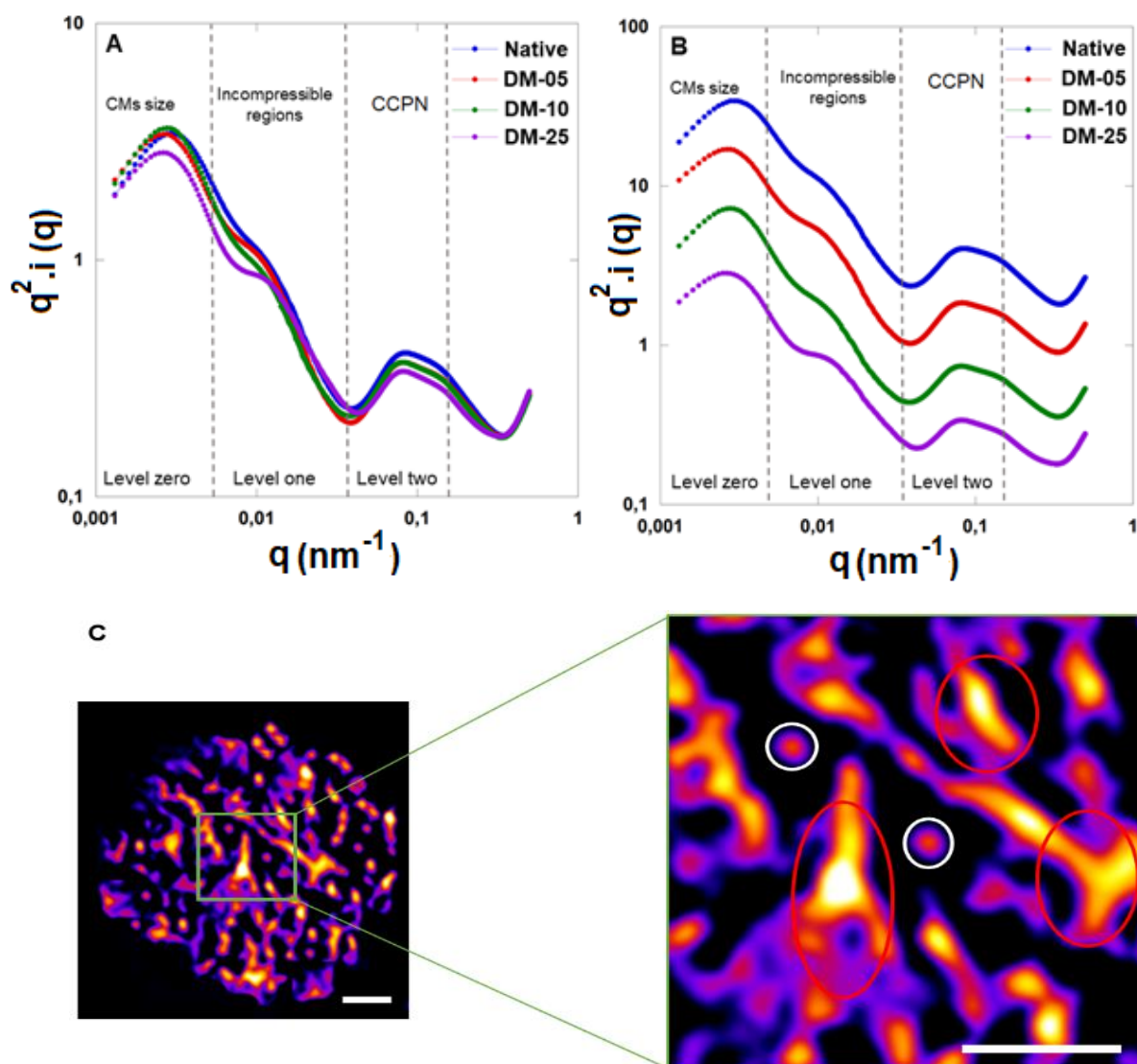


Figure 4 - Internal characterization obtained through Small Angle X-Ray Scattering (SAXS) of casein samples with different demineralization levels being: («native») = «native» casein; (DM-05) = 4.47% demineralized casein; (DM-10) = 9.16% demineralized casein; (DM-25) = 25.73% demineralized casein. (A) = SAXS spectra from all the samples, Results from an average of three repetitions and its duplicates. (B) = SAXS spectra from the separated samples*; * To obtain this graphic representation, the intensities were multiplied by a factor ($\sim \times 3$) only to present samples separately. (C) Schematic representation of an internal structure of a Cms, being the red circles representing the «Hard» structures that contain the CCP and the white circles the CCP present in the “void” regions, scale bar correspond to 50 nm. The three levels are represented in figure 4A, being: Level zero, which

corresponds to the CMs size; Level one, which represents the “hard” incompressible structures, and level two that are characteristic of the CCP region.

One can also notice, that such a relative decrease in the “shoulder” intensity correlates quite well with the relative decrease in the amount of phosphorous in the CCP clusters, which is detected by NMR as a function of the demineralization level. Indeed, as it is the case for the amount of organic and inorganic phosphorus measured by NMR (figure 3), from the «native» sample to DM-05. There is a significant loss of SAXS intensity for this “shoulder”, but not a loss as significant as for the other demineralized samples (DM-10 or DM-25).

Looking now at the second “shoulder,” the one associated with the so-called “Hard” structures (~10 to 40 nm) in the CM (Bouchoux et al., (2010), (Ingham et al., 2016). The detected decrease in intensity of this “shoulder” seems to be uncorrelated to the decrease in the intensity of the CCP “shoulder.” Indeed, upon comparing the «native» sample with DM-05, no remarkable changes in the intensity or the shape of the profile of the “Hard” structures has been observed. It seems that the substantial loss of CCPs detected by SAXS and NMR did not affect much of the micellar structure at this scale range. In contrast, passing from DM-05 to DM-10 and, subsequently, to DM-25, there is a small and progressive shift of the “shoulder” of these “Hard” structures to larger Q. These shifts indicate that in the samples with highest degree of demineralization, an internal reorganization of these “Hard” structures has been induced.

The interpretation concerning the last “shoulder,” the one at the largest scale and the lowest Q, is not possible from our data alone. Since this signal represents mixture of signals coming from the CM’s radius of gyration (the form factor of the CM) as well a change in the average inter-micellar particle distances in solution (the structure factor). This last factor is susceptible to change of micelle size, which will decrease the average inter-micellar distance in the solution and also with a change in stickiness and repulsiveness between the CMs, which will affect the distribution of inter-micellar distances in the solution.

4. Discussion

414 According to presented data in current study there is no significant modification
415 of the hydrophobic interactions between samples. It has been suggested that
416 hydrophobic interaction play a role in inter-protein interaction in casein (De Kruif, C.
417 G., 2014). Thus, the presented data suggest that demineralization did not change
418 much the protein-protein interactions in the samples.

419 Our data from current study also show that the measured loss of ions from CCP
420 (as detected by NMR) as well the decrease in attached phosphorylated residues
421 correlate quite well with the decrease of the P-CCP “shoulder” in SAXS data. This
422 observation agrees with the nanocluster model since, according to this model CCP
423 acts as a coordination center for the local protein network attached to it. Thus, in this
424 model the loss of the interaction between the phosphorylated center of casein and the
425 ions from the CPPs should always induce an observable loss of local protein network
426 around the CCPs.

427 In our study, NMR data indicate that the loss of ions from the CCPs does not decrease
428 the overall size of the CCPs but rather completely removes some CCPs from the
429 micelles leaving the remaining ones quite intact. This scenario is also supported by the
430 physical-chemistry of such objects (Bijl et al., 2019; Cross et al., 2005; Holt, C., 2004).
431 Indeed, the loss of the local protein network around CCPs means that some protein
432 “capping” the CCP have been detached. It has been clear from published work, that a
433 reduction in the amount of capping proteins around a nanocluster is rather a factor that
434 favors the instability of the CCP clusters (Bijl et al., 2019; Cross et al., 2005; Holt, C.,
435 2004). The fewer phosphorylated residues (from a protein or a peptide) “capping” a
436 CCP, the larger and unstable the CCP should be (Holt et al., 2004). Thus, it is unlikely
437 that the decrease in the amount of ions and sequestering proteins forming the P-CCPs
438 would induce a global decrease of the CCPs size. Rather than that, it is more likely
439 that the first clusters to lose ions (and the capping proteins) will become quickly
440 unstable leading to their complete excision from the micelles (agreement with NMR
441 data).

442 Indeed, this scenario is coherent with the fact that the presented NMR data do
443 not show a simple correlation between the total loss of calcium and phosphorus in
444 the samples and the specific loss of calcium and phosphate from the CCPs. The less
445 demineralized samples (DM-05 and DM-10) display a greater loss of these ions from
446 the CCPs (about 15% and 17% respectively) than the measured loss of calcium
447 phosphate in the samples (which is -5% and -10% respectively).

This means that there is a difference in equilibrium in terms of bound/free ions for the CCPs between the less demineralized samples and the most demineralized ones. Such change in equilibrium indicates a structural difference in the sequestered P-CCPs. In the «native» sample, CCPs are likely to be composed of some fraction (around 15-17%) of CCPs displaying fewer “capping” phosphorylated residues. Such CCPs are the first ones to be removed from the micelle by demineralization, since they are the less stable ones. This scenario explain quite well why NMR detected a less important loss of attached phosphorylated proteins in the less demineralized (comparing the «native» to the DM-05) samples than for the most demineralized ones (comparing the “DM-10” to the DM-25). Since the first clusters to be removed are likely to be the ones with less “capping” proteins, which explains their greater instability. Their depletion will generate a weaker loss of attached phosphorylated residues than the depletion of the more stable ones.

The data show, that the measured loss of ions from CCP (as detected by NMR) as well the decrease in attached phosphorylated residues correlate quite well with the decrease in intensity of the CCP “shoulder” in SAXS data (table 1). Noteworthy, a quasi-linear relation between the amount of proteins capping the phosphate centers and the intensity of the CCP “shoulder” observed in SAXS, in this demineralization range, is expected by the model used to interpret SAXS data (Ingham et al., 2016). This observation supports the nanocluster model view that all the CCP in the micelles acts as a cordination centers for the local protein network attached to it. Thus, in this model the loss of the interaction between the phosphorylated center of caseins and the ions from the CPPs should always induce a rather important loss of protein inhomogeneities around the CCPs.

	SAXS	
	loss in intensity of the CCP « shoulder » (%)	NMR Amount of P Ser (%)
« Native »	100	100
DM-05	92	93
DM-10	92	92
DM-25	80	84

Table 1. Comparison between the amount of attached phosphorous from phosphoserines (PSer) as quantified by NMR and the intensity of the CCP “shoulder”. The intensity of the “native” samples is considered as 100%.

In the literature, much of discussion about the composition, the structure and or the spatial distribution of the nanoclusters in the micelle have not considered the possibility of the presence of CCPs with different stabilities (Dalglish, 2011, Bhat, Dar, & Singh, 2016; Broyard & Gaucheron, 2015). Probably, the main reason for this is that most articles studying the evolution of the structure of CCP upon demineralization have been relying on the quantification of the evolution of the number of colloidal/free ions or/and structural data from SAXS or TEM (Bhat, Dar, & Singh, 2016; Broyard & Gaucheron, 2015; Dalglish, 2011; Dalglish & Law, 1989; Griffin, Silva, et al., 2013; Lyster, & Price, 1988; Udabage, McKinnon, & Augustin, 2000). From SAXS and TEM data alone is very hard to correlate the decrease in the micellar CCP content and the structural modification of the micelle and, so far at our knowledge, ³¹P NMR have not been used to studied samples with displaying a range of demineralized levels as it have been done in this work.

The question now is the relation between the depletion of those small-scale structures with the observed structural changes in a large scale “Hard” structures. Bouchoux et al.’s (2010) data indicate that the signal of those structures corresponds to large inhomogeneities in the CM. De Kruif, (2014)’s SAXS model did not take into account the “Hard Structure” “shoulder” observed in SAXS data, probably because SANS data in the same work (De Kruif, (2014) have showed that the micelles display a rather homogenous structures at medium to large scales (>8 nm). Nevertheless, more recent work (Ingham et al. 2016) have taken into account this shoulder in their model and concluded on the note that their data is consistent with the interpretation of Bouchoux et al. (2010): the intermediate-q feature is due to some medium scale inhomogeneities within the micelle (Ingham et al. 2016) which also is supported by cryo-TEM data (Trejo et al. 2011).

Ingham et al. (2016) have showed that the “Hard” region shoulder in SAXS data increases in intensity after some hours at 25°C, without any change in intensity elsewhere in the spectrum. Moreover, it has also been observed that micelles from different sources can display different intensities in this region (Day, L. et al., 2017). These data suggest a scenario where regions of the micelle could be re-structured to

form these “Hard regions” due to the destabilising factors such as calcium concentration, pH, temperature and time.

In highly demineralized samples (Ingham et al., 2016), the removal of 22% to 45% of minerals (addition of 5 mM and 10 mM of EDTA respectively) induces only very small changes in the SAXS signal of the “Hard” structure. One must conclude that there is a reasonable amount of proteins located in “Hard structures” and those proteins are not directly interacting with the CCP clusters, as the nanoclusters model would suggest, but rather they are stabilized by a larger protein-protein network. So any modification in the small scale structures (the P-CCPs) would not necessarily induce a change in such large scale inhomogeneity.

Indeed, in the present data, only the samples with higher degree of demineralization display a significant decrease in the intensity of these “Hard” regions. Thus, the observed local depletion of the P-CCP structures does have an almost any impact in the decrease of these large scale inhomogeneities. Indeed, for the less demineralized samples it is likely that the caseins previously attached to CCP, somehow still part of a large scale inter-protein network. In this way the excision of the CCP always strongly affect the small scale structure of the CM (the P-CCP centers) but it does not affect (at least for the less demineralized samples) as strongly, the large scale inhomogeneities. Thus, this specific behavior of “hard” region observed in this work is strong evidence that the micelles are composed of a medium scale protein-protein network generating these inhomogeneities.

5 CONCLUSIONS

This study aimed to evaluate the impact of the demineralization on the internal organization of the CMs structures of a dense casein micelle dispersion. Our data quite clearly indicate that demineralization does not induce a change in hydrophobicity of the micelle (at least at the demineralization levels studied), which suggests that no hydrophobic interactions substantial protein-protein reorganization occurs. It also shows that casein micelles display some clusters with strong stability than others indicating a structural heterogeneity in the complex CCPs (and proteins associated) found in the micelle. The loss of the less stable CCPs induces only a structural change at the smaller scale. In contrast, the loss the more stable clusters induce structural changes at the both, small as well at the medium scales. The data from current study

is an improvement in the sponge-like model described by Bouchoux et al., (2010) and at the same time adds more information about the role of the nanoclusters in keeping the structure of the micelle.

Acknowledgments

This research was supported by the French national center for scientific research (CNRS) attached to the project “ProteinoLAB,” a partnership between the Institut national de recherche pour l’agriculture, l’alimentation et l’environnement (INRAe) and Ingredia Dairy Experts. The authors also would like to say thanks to Ingredia dairy experts for the powder provided during this research.

5 Bibliography

- Antonio Fernandes de Carvalho, & Maubois, J.-L. (2010). Applications of Membrane Technologies in the Dairy Industry. In J. S. dos R. Coimbra & J. A. Teixeira (Eds.), *Engineering aspects of milk and dairy products* (First, pp. 33–56). Boca Raton: CRC Press.
- Bhat, M. Y, Dar, T. A & Singh, L. R (2016). Casein Proteins: Structural and Functional Aspects. In Gigli, I (Eds.), *Milk Proteins. From Structure to Biological Properties and Health Aspects*. IntechOpen
- Beliciu, C. M., Sauer, A., & Moraru, C. I. (2012). The effect of commercial sterilization regimens on micellar casein concentrates. *Journal of Dairy Science*, 95(10), 5510–5526. <https://doi.org/10.3168/jds.2011-4875>
- Bijl, E., Huppertz, T., van Valenberg, H., & Holt, C. (2019). A quantitative model of the bovine casein micelle: ion equilibria and calcium phosphate sequestration by individual caseins in bovine milk. *European Biophysics Journal*, 48(1), 45–59. <https://doi.org/10.1007/s00249-018-1330-2>
- Boiani, M., Fenelon, M., FitzGerald, R. J., & Kelly, P. M. (2018). Use of ³¹P NMR and FTIR to investigate key milk mineral equilibria and their interactions with micellar casein during heat treatment. *International Dairy Journal*, 81, 12–18. <https://doi.org/10.1016/j.idairyj.2018.01.011>
- Boiani, M., McLoughlin, P., Auty, M. A. E., FitzGerald, R. J., & Kelly, P. M. (2017). Effects of depleting ionic strength on ³¹P nuclear magnetic resonance spectra of micellar casein during membrane separation and diafiltration of skim milk. *Journal of Dairy Science*, 100(9), 6949–6961. <https://doi.org/10.3168/jds.2016-12351>
- Bouchoux, A., Debbou, B., Gésan-Guiziou, G., Famelart, M. H., Doublier, J. L., & Cabane, B. (2009). Rheology and phase behavior of dense casein micelle dispersions. *Journal of Chemical Physics*, 131(16), 1–12. <https://doi.org/10.1063/1.3245956>
- Bouchoux, Antoine, Gésan-Guiziou, G., Pérez, J., & Cabane, B. (2010). How to squeeze a sponge: Casein micelles under osmotic stress, a SAXS study. *Biophysical Journal*, 99(December), 3754–3762. <https://doi.org/10.1016/j.bpj.2010.10.019>

- Broyard, C., & Gaucheron, F. (2015). Modifications of structures and functions of caseins: a scientific and technological challenge. *Dairy Science and Technology*, 95(6), 831–862. <https://doi.org/10.1007/s13594-015-0220-y>
- Carvalho, A. F. de, & Maubois, J.-L. (2010). Applications of Membrane Technologies in the Dairy Industry. In J. S. dos R. Coimbra & J. A. Teixeira (Eds.), *Engineering aspects of milk and dairy products* (First Edit, pp. 33–52). Boca Raton: CRC Press.
- Corredig, M., & Dalgleish, D. G. (1996). Effect of temperature and pH on the interactions of whey proteins with casein micelles in skim milk. *Food Research International*, 29(1), 49–55. [https://doi.org/10.1016/0963-9969\(95\)00058-5](https://doi.org/10.1016/0963-9969(95)00058-5)
- Corredig, M., Nair, P. K., Li, Y., Eshpari, H., & Zhao, Z. (2019). Invited review: Understanding the behavior of caseins in milk concentrates. *Journal of Dairy Science*, 102(6), 4772–4782. <https://doi.org/10.3168/jds.2018-15943>
- Cross, K. J., Huq, N. L., Palamara, J. E., Perich, J. W., & Reynolds, E. C. (2005). Physicochemical characterisation of casein phosphopeptide-amorphous calcium phosphate nanocomplexes. *Journal of Biological Chemistry*, 280(15), 15362–15369. <https://doi.org/10.1074/jbc.M413504200>
- Crowley, S. V., Megemont, M., Gazi, I., Kelly, A. L., Huppertz, T., & O'Mahony, J. a. (2015). Rehydration characteristics of milk protein concentrate powders. *Journal of Food Engineering*, 149, 105–113. <https://doi.org/10.1016/j.idairyj.2014.03.005>
- Crowley, S. V., Megemont, M., Gazi, I., Kelly, A. L., Huppertz, T., & O'Mahony, J. A. (2014). Heat stability of reconstituted milk protein concentrate powders. *International Dairy Journal*, 37(2), 104–110. <https://doi.org/10.1016/j.idairyj.2014.03.005>
- Dahbi, L., Alexander, M., Trappe, V., Dhont, J. K. G., & Schurtenberger, P. (2010). Rheology and structural arrest of casein suspensions. *Journal of Colloid and Interface Science*, 342(2), 564–570. <https://doi.org/10.1016/j.jcis.2009.10.042>
- Dalgleish, D. G. (2011). On the structural models of bovine casein micelles—review and possible improvements. *Soft Matter*, 2265, 7(6).
- Dalgleish, D. G & Law, A. J. R. (1989). pH-Induced dissociation of bovine casein micelles II. Mineral solubilization and its relation to casein release. *Journal of Dairy Research*, 727-735.
- Day, L., Raynes, J. K., Leis, A., Liu, L. H., & Williams, R. P. W. (2017). Probing the internal and external micelle structures of differently sized casein micelles from

individual cows milk by dynamic light and small-angle X-ray scattering. *Food Hydrocolloids*, 69, 150–163. <https://doi.org/10.1016/j.foodhyd.2017.01.007>

De Kruif, C. G. (2014). The structure of casein micelles: A review of small-angle scattering data. *Journal of Applied Crystallography*, 47(5), 1479–1489. <https://doi.org/10.1107/S1600576714014563>

De Kruif, C. G., & Zhulina, E. B. (1996). K-Casein As a Polyelectrolyte Brush on the Surface of Casein Micelles. *Colloids and Surfaces A: Physicochemical and Engineering Aspects*, 117(1–2), 151–159. [https://doi.org/10.1016/0927-7757\(96\)03696-5](https://doi.org/10.1016/0927-7757(96)03696-5)

de Kruif, C.G. (1998). Supra-aggregates of Casein Micelles as a Prelude to Coagulation. *Journal of Dairy Science*, 81(11), 3019–3028. [https://doi.org/10.3168/jds.S0022-0302\(98\)75866-7](https://doi.org/10.3168/jds.S0022-0302(98)75866-7)

De Kruif, C.G, & Holt, C. (2003). Casein micelle structure, functions and interaction. In P.F. Fox & P. L. H. McSweeney (Eds.), *Advances in Dairy Chemistry* (3rd ed., Vol. 1, pp. 233–276). Kluwer Academic/Plenum Publishers.

de Kruif, Cornelis G., Huppertz, T., Urban, V. S., & Petukhov, A. V. (2012). Casein micelles and their internal structure. *Advances in Colloid and Interface Science*, 171–172, 36–52. <https://doi.org/10.1016/j.cis.2012.01.002>

De Sa Peixoto, P., Silva, J. V. C., Laurent, G., Schmutz, M., Thomas, D., Bouchoux, A., & Gésan-Guizieu, G. (2017). How High Concentrations of Proteins Stabilize the Amorphous State of Calcium Orthophosphate: A Solid-State Nuclear Magnetic Resonance (NMR) Study of the Casein Case. *Langmuir*, 33(5), 1256–1264. <https://doi.org/10.1021/acs.langmuir.6b04235>

Famelart, M. H., Gauvin, G., Pâquet, D., & Brulé, G. (2009). Acid gelation of colloidal calcium phosphatedepleted preheated milk. *Dairy Science and Technology*, 89(3–4), 335–348. <https://doi.org/10.1051/dst/2009014>

Frédéric Gaucheron. (2005). The minerals of milk. *Reproduction Nutrition Development*, 45, 473–483. <https://doi.org/10.1051/rnd>

Gardiennet-Doucet, C., Assfeld, X., Henry, B., & Tekely, P. (2006). Revealing successive steps of deprotonation of L- Phosphoserine through ^{13}C and ^{31}P chemical shielding tensor fingerprints. *Journal of Physical Chemistry A*, 110(29), 9137–9144. <https://doi.org/10.1021/jp062184v>

Gonzalez-Jordan, A., Thomar, P., Nicolai, T., & Dittmer, J. (2015). The effect of pH on the structure and phosphate mobility of casein micelles in aqueous solution.

Food Hydrocolloids, 51, 88–94. <https://doi.org/10.1016/j.foodhyd.2015.04.024>

Holt C. (2004). An equilibrium thermodynamic model of the sequestration of calcium phosphate by casein micelles and its application to the calculation of the partition of salts in milk. *Eur Biophys* 33(5), 421-34. <https://doi.org/10.1007/s00249-003-0377-9>

Horne, D. S. (2017). A balanced view of casein interactions. *Current Opinion in Colloid and Interface Science*, 28, 74–86. <https://doi.org/10.1016/j.cocis.2017.03.009>

Ingham, B., Smialowska, A., Erlangga, G. D., Matia-Merino, L., Kirby, N. M., Wang, C., ... Carr, A. J. (2016). Revisiting the interpretation of casein micelle SAXS data. *Soft Matter*, 12(33), 6937–6953. <https://doi.org/10.1039/C6SM01091A>

International Euromonitor. (2018). *Trends and Drivers of the Sports Nutrition Industry*.

Kinematica AG. (2013). *POLYTRON® PT 10-35 GT- Operator manual* (Vol. 1). Lizersn - Switzerland.

Kort, E. De, Minor, M., Snoeren, T., Hooijdonk, T. Van, & Linden, E. Van Der. (2011). Effect of calcium chelators on physical changes in casein micelles in concentrated micellar casein solutions. *International Dairy Journal*, 21(12), 907–913. <https://doi.org/10.1016/j.idairyj.2011.06.007>

Luo, X., Vasiljevic, T., & Ramchandran, L. (2016). Effect of adjusted pH prior to ultrafiltration of skim milk on membrane performance and physical functionality of milk protein concentrate. *Journal of Dairy Science*, 99(2), 1083–1094. <https://doi.org/10.3168/jds.2015-9842>

Massiot, D., Fayon, F., Capron, M., King, I., Le Calvé, S., Alonso, B., ... Hoatson, G. (2002). Modelling one- and two-dimensional solid-state NMR spectra. *Magnetic Resonance in Chemistry*, 40(1), 70–76. <https://doi.org/10.1002/mrc.984>

McCarthy, N. A., Power, O., Wijayanti, H. B., Kelly, P. M., Mao, L., & Fenelon, M. A. (2017). Effects of calcium chelating agents on the solubility of milk protein concentrate. *International Journal of Dairy Technology*, 70, 1–9. <https://doi.org/10.1111/1471-0307.12408>

Nogueira, M. H., Ben-harb, S., Schmutz, M., Doumert, B., Nasser, S., Derensy, A., ... Peixoto, P. P. S. (2020). Multiscale quantitative characterization of demineralized casein micelles : How the partial excision of nano-clusters leads to the aggregation during rehydration. *Food Hydrocolloids*, 105(February), 105778. <https://doi.org/10.1016/j.foodhyd.2020.105778>

- Peixoto, P. D. S., Bouchoux, A., Huet, S., Madec, M. N., Thomas, D., Floury, J., & Gésan-Guizieu, G. (2015). Diffusion and partitioning of macromolecules in casein microgels: Evidence for size-dependent attractive interactions in a dense protein system. *Langmuir*, 31(5), 1755–1765. <https://doi.org/10.1021/la503657u>
- Pierre, A., Fauquant, J., Graet, Y. Le, Piot, M., & Maubois, J. (1992). Préparation de phosphocaséinate natif par microfiltration sur membrane To cite this version : *Le Lait*, 72, 461–474.
- Ramchandran, L., Luo, X. X., & Vasiljevic, T. (2017). Effect of chelators on functionality of milk protein concentrates obtained by ultrafiltration at a constant pH and temperature. *Journal of Dairy Research*, 84(4), 471–478. <https://doi.org/10.1017/S0022029917000528>
- Schuck, P., Piot, M., Graet, Y. Le, Fauquant, J., Brul, G., Graet, Y. Le, & Fauquant, J. (1994). Déshydratation par atomisation de phosphocaséinate natif obtenu par microfiltration sur membrane.
- Silva, N. N., Piot, M., de Carvalho, A. F., Violleau, F., Fameau, A. L., & Gaucheron, F. (2013). PH-induced demineralization of casein micelles modifies their physico-chemical and foaming properties. *Food Hydrocolloids*, 32(September 2015), 322–330. <https://doi.org/10.1016/j.foodhyd.2013.01.004>
- Trejo, R., Dokland, T., Jurat-Fuertes, J., Harte, F. (2011). Cryo-transmission electron tomography of native casein micelles from bovine milk. *Journal of Dairy Science*, (94/12), 5770-5775. <https://doi.org/10.3168/jds.2011-4368>
- Walstra, P., Wouters, J. T. M., & Geurts, T. J. (2006). *Dairy Science and Technology*. (T. & F. Group, Ed.) (Second). Boca Raton: CRC. <https://doi.org/10.1177/1082013205052515>